AGU PUBLICATIONS

JGR

Journal of Geophysical Research: Biogeosciences

RESEARCH ARTICLE
10.1002/2017JG004084

Key Points:
- Physical processes, such as entrainment and density currents, are essential model elements for accurate simulation of lake carbon dynamics
- Dissolved organic carbon decay was less sensitive to temperature than is commonly assumed

Supporting Information:
- Supporting Information S1

Correspondence to:
O. Hararuk,
ohararuk@gmail.com

Citation:
Hararuk, O., Zwart, J. A., Jones, S. E., Prairie, Y., & Solomon, C. T. (2018). Model-data fusion to test hypothesized drivers of lake carbon cycling reveals importance of physical controls. *Journal of Geophysical Research: Biogeosciences*, *123*, 1130–1142. https://doi.org/10.1002/2017JG004084

Received 31 JUL 2017
Accepted 26 FEB 2018
Accepted article online 2 MAR 2018
Published online 30 MAR 2018

Model-Data Fusion to Test Hypothesized Drivers of Lake Carbon Cycling Reveals Importance of Physical Controls

Oleksandra Hararuk[1,2], Jacob A. Zwart[3], Stuart E. Jones[3], Yves Prairie[4], and Christopher T. Solomon[2]

[1]Department of Natural Resource Sciences, McGill University, Montréal, Quebec, Canada, [2]Cary Institute of Ecosystem Studies, Millbrook, NY, USA, [3]Department of Biological Sciences, University of Notre Dame, Notre Dame, IN, USA, [4]Département des sciences biologiques, Université du Québec à Montréal, Montréal, Quebec, Canada

Abstract Formal integration of models and data to test hypotheses about the processes controlling carbon dynamics in lakes is rare, despite the importance of lakes in the carbon cycle. We built a suite of models (n = 102) representing different hypotheses about lake carbon processing, fit these models to data from a north-temperate lake using data assimilation, and identified which processes were essential for adequately describing the observations. The hypotheses that we tested concerned organic matter lability and its variability through time, temperature dependence of biological decay, photooxidation, microbial dynamics, and vertical transport of water via hypolimnetic entrainment and inflowing density currents. The data included epilimnetic and hypolimnetic CO_2 and dissolved organic carbon, hydrologic fluxes, carbon loads, gross primary production, temperature, and light conditions at high frequency for one calibration and one validation year. The best models explained 76–81% and 64–67% of the variability in observed epilimnetic CO_2 and dissolved organic carbon content in the validation data. Accurately describing C dynamics required accounting for hypolimnetic entrainment and inflowing density currents, in addition to accounting for biological transformations. In contrast, neither photooxidation nor variable organic matter lability improved model performance. The temperature dependence of biological decay (Q10) was estimated at 1.45, significantly lower than the commonly assumed Q10 of 2. By confronting multiple models of lake C dynamics with observations, we identified processes essential for describing C dynamics in a temperate lake at daily to annual scales, while also providing a methodological roadmap for using data assimilation to further improve understanding of lake C cycling.

1. Introduction

Of the carbon (C) loaded to inland waters at a global scale, 50–60% evades to the atmosphere, ~20% is buried, and only 25–30% is transported downstream to the oceans (Raymond et al., 2013; Tranvik et al., 2009). Lakes, streams, and other freshwater ecosystems are thus globally significant hotspots for carbon transformation and storage, burying or emitting nearly 3 Pg C $year^{-1}$, an amount similar in magnitude to the global terrestrial C sink (Le Quéré et al., 2016). These integrated global estimates mask information about the controls of freshwater carbon cycling, which is essential for estimating C transformation and storage rates under changing environmental conditions. The importance of C cycling controls is evident from the huge variability in the fate of carbon among individual lake ecosystems. For instance, C burial rates in lakes can vary 1,000-fold within a relatively small geographic region, and the proportion of the C load to a lake that is emitted to the atmosphere varies from 1% to as much as 75% (Einola et al., 2011; Tranvik et al., 2009).

Making sense of the variability in C dynamics is essential for understanding carbon processing in lakes and predicting future carbon balances. Previous studies demonstrate the wide range of processes that can impact lake carbon cycling and emissions, like the lability of organic matter and how it changes through time (del Giorgio & Davis, 2003; Guillemette & del Giorgio, 2011; Middelburg et al., 1993), the temperature dependence of microbial respiration (del Giorgio & Davis, 2003; Guillemette & del Giorgio, 2011; Middelburg et al., 1993), photooxidation (Amado et al., 2003; Cory et al., 2014; Molot & Dillon, 1997; Shiller et al., 2006), physical processes like mixing and stratification (Bower & McCorkle, 1980; C. A. Kelly et al., 2001; Rueda et al., 2007; Vachon & del Giorgio, 2014), and many others. Yet it is not clear which of these processes are essential for accurately describing or predicting carbon dynamics.

Efforts to model lake carbon cycles have generally assumed a priori which processes should be represented in the model, and then estimated (formally or informally) the parameters of that fixed model structure, rather than treating the model structure as a set of hypotheses to be tested. Consequently, we lack evidence-based guidance on what mechanisms should be included in lake carbon biogeochemistry models, and perhaps the performance of past models has suffered as a result. For instance, some models which have assumed temperature-sensitive decay of a single, uniformly labile dissolved organic carbon (DOC) pool have been able to reproduce observed annual average carbon stocks, but produced substantial mismatches to observed seasonal dynamics (Cardille et al., 2007; Hanson et al., 2004). Another model added variable lability and photooxidation to a temperature-sensitive decay model, but often deviated from in situ observations despite its ability to describe DOC dynamics in lab incubations (Vachon, Solomon et al., 2017). Rigorous, hypothesis-driven integration of models with data would allow clear tests of the importance of proposed mechanisms and robust estimates of process rates and improve our ability to describe and predict carbon dynamics in lakes. In this study we used a data assimilation approach to test hypotheses about the processes essential for accurately representing C dynamics in a lake ecosystem. We considered biotic and abiotic processes that are known or thought to have important effects on C processing in lakes, including variable lability of organic carbon (Guillemette & del Giorgio, 2011), temperature dependence of biological decay (Yvon-Durocher et al., 2012), photooxidation (Vachon, et al., 2016), microbial dynamics (Middelboe & Lundsgaard, 2003), and vertical transport of water via hypolimnetic entrainment (Jennings et al., 2012) and inflowing density currents (Rueda et al., 2007). We used a Bayesian Markov chain Monte Carlo approach, and two years of data from a dimictic north temperate lake, to parameterize a large suite of models, which included various combinations of our hypothesized processes. We determined which processes were essential to include in the model in order to accurately represent carbon dynamics and asked whether fitted estimates of key parameters were consistent with previous estimates derived from other systems and approaches.

2. Methods

We aimed to identify model structural assumptions (described in more details in the supporting information) that were critical for good representation of epilimnetic C dynamics in situ. We built 102 models with various combinations of the structural assumptions and calibrated them against the observations of epilimnetic DOC and CO_2 content collected from a small north temperate lake in 2014. After calibrating the model parameters, we evaluated model performance on a validation portion of the observations, which were collected in 2015. We performed model analyses in R and provide code at https://github.com/MFEh2o/Hararuk_DA.

2.1. Observed Data

The study lake—Long Lake—is located at the University of Notre Dame Environmental Research Center (46°13′N 89°32′W). Its area is 8.1 ha, and its mean depth is 3.8 m. The hourglass-shaped lake was divided at its narrow part by an impermeable curtain (Curry Industries) as a part of an in situ manipulative experiment that explored the effects of elevated DOC on lake biogeochemistry and biota (P. T. Kelly et al., 2016; Zwart et al., 2016). We focused on modeling C dynamics in the treatment portion of the lake (East Long Lake; area = 3.2 ha), because the surface inlet to the lake enters that basin and therefore we were able to constrain DOC inputs to that basin well. East Long Lake is a dimictic, mesotrophic (total phosphorus: 15.9 $\mu g\ L^{-1}$; chlorophyll-a: 7.9 $\mu g\ L^{-1}$) lake with a water residence time of 296 days (Zwart et al., 2016, 2017). Light is attenuated fairly quickly in the water column of East Long Lake (light extinction coefficient: 2.86 m^{-1}) due to the high concentration of DOC (Table 1). The lake is ice-covered annually and thermally stratifies shortly after ice out, which typically occurs in April or early May.

Water from the epilimnion and hypolimnion was sampled weekly from May to October of 2014 and 2015 and analyzed for DOC, dissolved inorganic carbon (DIC), and CO_2 content. We measured DOC on the filtrate of lake water passing through precombusted (450°C for 4 hr) GF/F filters using a total organic carbon analyzer (TOC-V; Shimadzu Scientific Instruments). For DIC and CO_2 sample analysis, we collected water with a 60 mL syringe and an airtight valve either by submerging the syringe to the sampling depth for shallow samples ($<$0.25 m) or by extracting water from a Van Dorn sampler for deeper samples. Upon returning to the lab, 0.1 mL of 4N H_2SO_4 was added to the DIC sampling syringes to convert all inorganic carbon to CO_2. N_2 gas headspace (30 and 10 mL) were added to 30 mL of water in each DIC and CO_2 syringe, respectively, and the syringes were shaken vigorously for at least 90 s and then rested for 10 min to allow for headspace

Table 1
Characteristics of East Long Lake in 2014 and 2015

Variable	Description	2014	2015
V	Volume, m^3	128,700	128,700
A	Area, m^2	32,000	32,000
Qin	Inlet stream discharge, m^3/season	30,000	22,000
PPT	Precipitation, m^3/season	13,000	11,000
Qout	Outlet and groundwater discharge, m^3/season	117,000	15,000
PAR	Average photosynthetically active radiation, mol photons/m^2/day	37.00	36.62
depth_t	Average thermocline depth, m	2.34	2.46
T	Mean epilimnetic temperature, °C	21.45	21.80
DOC_stream	Average dissolved organic carbon (DOC) concentration in stream, mg/L	66.00	48.00
CO_2_stream	Average CO_2 concentration in stream, mg/L	5.26	4.98
DOC_precip	DOC concentration in precipitation, mg/L	3.20	3.20
DOC_epi	Average DOC in the epilimnion, mg/L	10.52	9.86
DOC_hypo	Average DOC in the hypolimnion, mg/L	11.31	11.98
CO_2_epi	Mean epilimnetic CO_2, mg/L	0.38	0.42
DIC_hypo	Mean hypolimnetic DIC, mg/L	6.30	5.96
ph_epi	pH of epilimnetic water	5.95	6.10
ph_hypo	pH of hypolimnetic water	4.90	5.30

equilibration. The headspace was analyzed for CO_2 on a gas chromatograph (Agilent 6890; Agilent Technologies), and we converted analyzed headspace CO_2 concentrations to dissolved in the water using Henry's law constant. Although CO_2 was not measured in the hypolimnion, based on pH (Table 1), we estimated that 90–95% of the measured hypolimnetic DIC was in CO_2 form (Stumm & Morgan, 1981).

Temperature profiles were recorded every 10 min using a fixed thermistor chain (Onset HOBO Pendants; Onset Computer Corporation). Incident photosynthetically active radiation (PAR) was also measured every 10 min from a floating platform (Onset HOBO met station, Onset Computer Corporation). Water height in the inlet stream was measured every 10 min with a pressure sensor (Onset HOBO U20-001-04 Water Level Data Logger; Onset Computer Corporation) behind a 90° V notch weir (Daugherty & Ingersoll, 1954), and stream discharge (Q) was estimated using equation (1):

$$Q = \frac{8}{15} \times \sqrt{2g} \times \tan\left(\frac{\theta}{2}\right) \times H^{5/2} \quad (1)$$

where g is the acceleration due to gravity (9.81 $m^2\ s^{-1}$), θ is the angle of the V notch (90° for our weir), and H was water height in the V notches. The stage-discharge relationship was confirmed using salt slug injection, dilution-gauging (Moore, 2005). Stream carbon concentrations (DOC, DIC, and CO_2) were linearly interpolated to discharge measurement frequency and multiplied by stream discharge to estimate inlet stream carbon flux to the lake. Although there was a weak negative relationship between inlet stream discharge and DOC concentration, inlet stream DOC concentration was highly autocorrelated (significantly autocorrelated at weekly sampling intervals); thus, linear interpolation between DOC measurements was appropriate.

Rainfall was measured hourly with a tipping bucket rain gauge (TE525MM-L; Campbell Scientific, Inc.), whereas the DOC and CO_2 concentrations in rainwater were measured twice over the sampling period; therefore, the average concentrations were used to estimate DOC and CO_2 input with rain (Zwart et al., 2016). Monthly measurements of groundwater discharge showed that the lake perpetually loses water to the regional aquifer; we used average groundwater discharge values to estimate DOC and CO_2 flux to groundwater. Groundwater discharge was estimated using nine in-lake piezometers. Hydraulic head (h; vertical distance between water level in each piezometer and lake water level) was measured at least monthly and values were averaged across the sampling period since temporal heterogeneity was low. Hydraulic conductivity (k) was estimated for each piezometer using slug tests (Bouwer, 1989), and specific groundwater discharge (q) was estimated using Darcy's law:

$$q = k \times \left(\frac{h}{l}\right) \times a \quad (2)$$

where l is the piezometer insertion depth (vertical distance from the top of lake sediments to the top of piezometer screen opening) and a is the piezometer cross-sectional area. All measurements of hydraulic head were negative, meaning that groundwater was flowing from the lake to the groundwater aquifer (recharge). Whole-lake groundwater recharge was estimated as the product of the mean of all negative piezometer q and lake sediment area over which recharge was observed. Groundwater discharge for our study lake was small as it constituted less than 4% of hydrologic outflow. Outflow of carbon from the lake was estimated as the product of q_{out} and lake carbon concentration.

Gross primary production was estimated from 10 min dissolved oxygen (DO) measurements (YSI 6600 V2 Sonde, YSI Incorporated) by fitting a maximum likelihood metabolism model to the high-frequency DO cycles as described by Solomon et al. (2013). More information on methods and frequency of data collection and estimation is given in Zwart et al. (2016).

2.2. Model Structures

We simulated dynamics of the epilimnetic DOC and CO_2 as a system of first-order linear differential equations, which can be summarized as

$$\frac{dX}{dt} = I(t) - A(t)X(t) \tag{3}$$

where $X(t)$ is a vector of epilimnetic DOC and CO_2 pools at the time t; $I(t)$ is the vector of inputs to the DOC and CO_2 pools, which included stream, precipitation, and overland flow; and $A(t)$ is the decay and transfer matrix. The $A(t)$ matrix included the effects of biotic and abiotic factors on DOC mineralization, hydrologic export, atmospheric exchanges, and fluxes to or from the hypolimnion (depending on the change in thermocline depth).

The structural assumptions tested in this study were related to the size of $X(t)$, elements of $I(t)$, and $A(t)$. For instance, we tested whether accounting for varying DOC lability (by modeling both recalcitrant and labile forms, thus adding a third row to the $X(t)$ vector and changing the other terms of equation (3) accordingly) improved model performance. We tested whether density differences between stream and epilimnetic water led to partitioning of inflowing C between the epilimnion and hypolimnion, by modifying elements of $I(t)$ by a function $f(\Delta\rho)$, which allocated less stream C to the epilimntion with increasing density gradient $\Delta\rho$. We tested the effect of photooxidation by modifying elements of $A(t)$ by a coefficient, which was set to be a function of photosynthetically active radiation, f(PAR). If the model formulation included entrainment C fluxes, we explored whether there was a gradient in hypolimnetic DOC and CO_2 concentrations. If the model formulation accommodated varying DOC recalcitrance, we modified $I(t)$ to test whether change in the allochthonous recalcitrance midseason would improve model performance and altered $A(t)$ to test whether model would improve if recalcitrant DOC contributed to the labile DOC pool during oxidation. Some structural assumptions were mutually exclusive (e.g., models with one DOC pool versus models with two DOC pools), but most were not, overall yielding 102 models. For detailed model descriptions and mutual exclusivity of the assumptions please refer to the supporting information.

We split the observations from East Long Lake into two groups: the observations that were collected in 2014 were used to calibrate the models' parameters and the observations that were collected in 2015 were used to evaluate the performance of the models with calibrated parameters. Such design helped avoid overfitting of models, ensuring that the best fitting models captured the signal rather than noise in the observations.

2.3. Bayesian Inversion

We calibrated the model parameters using a Bayesian Markov chain Monte Carlo technique (Besag et al., 1995). The prior distributions for the parameters were assumed to be uniform. We sampled from the posterior parameter distribution by proposing a set of parameters and accepting or rejecting it using the Metropolis criterion (Spall, 2005). For the first 10,000 iterations the proposal distribution was uniform, afterwards we calculated a parameter covariance matrix, and switched the parameter proposal distribution to the multivariate normal as in Xu et al. (2006) for the next 490,000 simulations:

$$c^{new} = N\left(c^{k-1}, C_k\right) \tag{4}$$

where C_k is defined as in Haario, et al. (2001):

$$C_k = \begin{cases} C_0 & k = 10,000 \\ s_d \,\mathrm{cov}\left(c^0, \ldots, c^{k-1}\right) & k > 10,000 \end{cases} \quad (5)$$

where $s_d = 2.38/\sqrt{n}$ and n is the number of parameters in a model (Gelman, et al., 1996) and C_0 is the parameter covariance matrix constructed from the first 10,000 iterations. The rates of parameter acceptance were 15–30%, indicating good mixing, which is necessary to arrive at stable posterior distributions. We discarded the first half of the accepted parameters as a "burn-in" period and sampled 3,000 estimates from the second half of the accepted parameters to generate the marginal posterior parameter distributions and calculate the maximum likelihood parameter values.

2.4. Identifying Important Elements of Model Structure

We measured the goodness of model performance by the Akaike information criterion (AIC) (Akaike, 1974), which was calculated from the model output for 2015 validation data as

$$\mathrm{AIC} = 2n - 2\ln\left(\widehat{L}\right) \quad (6)$$

where n is the number of parameters in a model and $\widehat{L}$ is the maximized likelihood function obtained during Bayesian inversion. With 102 model formulations, identifying processes that consistently improved model performance was not trivial; therefore, we decided to explore the trends in model performance by representing AIC values as a function of the presence of processes and particular structural assumptions. We used a machine learning technique, recursive partitioning by conditional inference (Hothorn et al., 2006), to find the patterns in AIC values. Unlike many recursive partitioning methods, conditional inference trees do not overfit the models and are not biased toward covariates with many possible splits. This method is available in R "partykit" package (Hothorn et al., 2015), which we used to analyze AIC values in our study.

3. Results

3.1. Lake Characteristics

Lake characteristics varied between 2014 and 2015, the calibration and validation years. Year 2015 was a drier year than 2014: there was 25% less inlet stream discharge, 15% less rainfall, and 87% less outlet and groundwater discharge during the measurement period (Table 1). There was also 15% (or 506 mm) less snowfall during the October 2014 to May 2015 period (which contributed to the 2015 stream discharge) than during the same period in 2013–2014 (data from the nearest station with available measurements published at https://www.ncdc.noaa.gov/cdo-web/). It is important to note that drastic differences between 2014 and 2015 water discharge were partly due to the timing of the measurements: in 2014 we started the measurements shortly after snowmelt, capturing the resulting outlet discharge without some of the corresponding high inlet discharge. The epilimnion was slightly deeper and warmer in 2015 than 2014. Stream DOC and CO_2 concentrations were 27% and 5% lower, respectively, in 2015 than in 2014, which together with reduced stream discharge resulted in 50% and 42% smaller stream DOC and CO_2 load in 2015. On average, there was slightly less DOC in the epilimnion in 2015 than in 2014; however, hypolimnetic DOC concentration was slightly increased. Despite the lower loads, epilimnetic CO_2 was slightly higher in 2015, whereas hypolimnetic DIC was slightly lower.

3.2. Important Processes and Structural Assumptions

We calibrated 102 model formulations against the 2014 observations of DOC and CO_2, validated the models against the 2015 DOC and CO_2 observations, and evaluated their performance against the 2015 data using AIC. AIC varied widely across the model formulations, indicating that model assumptions were an important determinant of model performance (Figure 1). The conditional inference tree analysis identified a cluster of 20 model formulations that exhibited significantly better performance than all other models (Figure 1). The best performing models simulated entrainment, assumed a depth gradient in hypolimnetic CO_2 concentrations, and modeled epilimnetic DOC and CO_2 loads as a function of density differences between stream and epilimnetic water. Within the cluster of 20 best performing models were models that assumed two DOC pools (i.e., labile and recalcitrant) or just one, presence or absence of photooxidation of DOC, presence or absence of a depth gradient in hypolimnetic DOC concentration, dependence or independence of labile DOC on

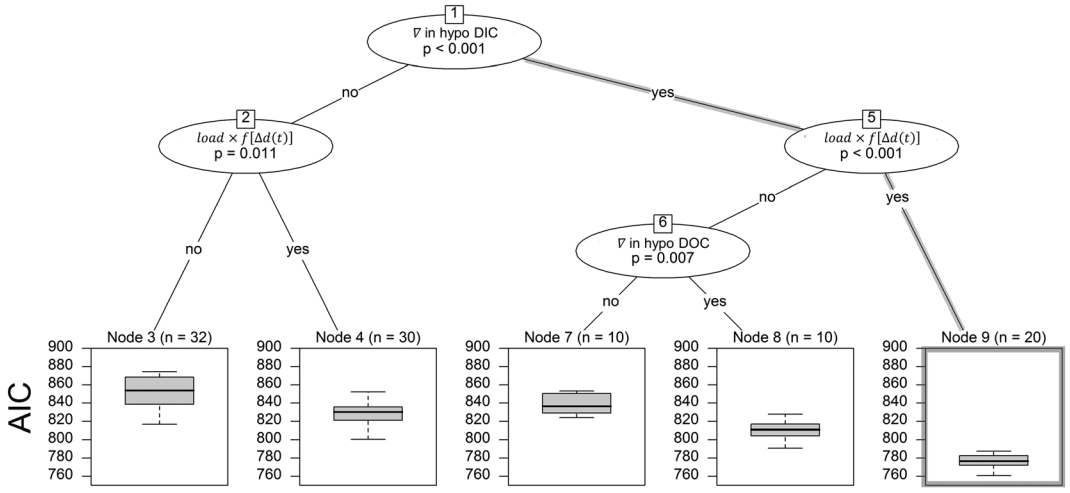

Figure 1. Processes and structural assumptions that significantly improved models' Akaike information criterion (AIC). "Yes" and "no" indicate presence or absence of a process or assumption in a model. The thick gray lines highlight a path to a cluster of best performing models (Node 9). ∇ in hypoDIC signifies the assumption that hypolimnetic dissolved inorganic carbon (DIC) concentrations were nonuniform across depth; load × $f[\Delta d(t)]$ indicates that stream loads of dissolved organic carbon (DOC) and CO_2 are partitioned between the epilimnion and the hypolimnion as a function of the water density (temperature) difference between the stream and the epilimnion. In the Node 3 two AIC outliers with values 1025.9 and 1041.8 are masked in order to reduce the range of *y* axes and make differences between the nodes more apparent.

recalcitrant DOC decay, and variable or constant incoming DOC quality. Such variety among the best performing models indicates that these processes did not affect the dynamics of epilimnetic DOC and CO_2 as much as did entrainment, the depth gradient in hypolimnetic CO_2 concentration, and the density-dependent partitioning of incoming DOC and CO_2 between epilimnion and hypolimnion.

3.3. Best Models

3.3.1. Structure and Performance

The four best performing models had similar structures and performance; all four simulated one DOC pool, and their AIC ranged from 761 to 771. All four of these models, like the others in the cluster of the top 20 models, included entrainment, a depth gradient in hypolimnetic DIC, and density-dependent input partitioning of DOC and CO_2 load. The differences among the four models were in the presence of photooxidation and the assumption of a depth gradient in hypolimnetic DOC. The top four models explained a substantial portion of the variability in the epilimnetic CO_2 and DOC concentration in the validation data set (76–81% and 63–67%, respectively; Figure 2). Most observations were within ±2 SD of the mean predicted value. For more detailed description of model assumptions, refer to the supporting information.

3.3.2. Parameter Values

We evaluated whether posterior distributions of the parameters were similar across the models and examined the models' ability to reproduce epilimnetic C dynamics in 2015 (the validation year). Most parameters in the top four models were well constrained relative to their priors (expressed as the *x* axis range in Figure 3 and Table S1).

The fitted models emphasized that physical processes—including density-dependent partitioning of stream inputs between the epilimnion and the hypolimnion as well as entrainment of hypolimnetic water—are important for understanding epilimnetic C dynamics in this system. The calibrated values of k_{dens} (Figure 3c and Table S1) were significantly higher than 0, indicating a distinct influence of the density difference between stream and epilimnetic water on the partitioning of DOC and CO_2 inputs between epilimnion and hypolimnion. Calibrated values for u_2, an entrainment-related parameter that tested the presence of a depth gradient in hypolimnetic DOC, converged to 0.85 (Figure 3g and Table S1), which indicated a near-uniform depth distribution of hypolimnetic DOC. On the other hand, u_1, the parameter that tested if there was a gradient in hypolimnetic CO_2, varied from 0.14 to 0.19 among the four best performing models (Figure 3f and Table S1), which indicated a distinct depth gradient in hypolimnetic CO_2 concentrations.

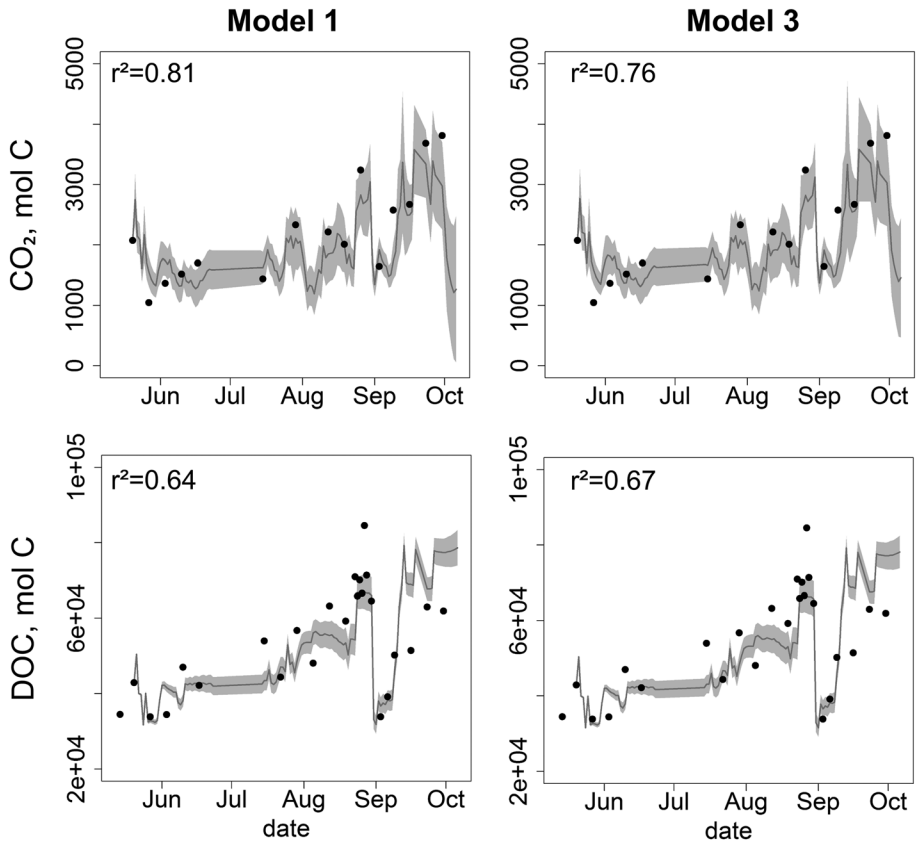

Figure 2. Performance of the best models in representing epilimnetic (first row) CO_2 and (second row) dissolved organic carbon (DOC) in 2015. The gray shaded region is model predictions ±2 standard deviations; the black dots are observed data points. Model 2 and 4 exhibited similar performance and are not shown. Model 1 and 3 are similar in structure (one DOC pool, density gradient-dependent C partitioning between epilimnion and hypolimnion, with entrainment and depth gradient in hypolimnetic dissolved inorganic carbon) with the exception that Model 3 simulates photooxidation. DOC concentrations ranged from 0.6 to 1.1 mmol L^{-1}, and CO_2 concentrations ranged from 0.005 to 0.05 mmol L^{-1}.

The low estimates of u_1 indicated that the CO_2 concentrations were higher at the bottom than near the top of the hypolimnion, which is commonly observed in hypoxic lakes (Fahrner et al., 2008; Rinta et al., 2015).

All four of the best models estimated similar total rates of DOC decay, although estimates of the biological decay (k_{20}) varied depending on whether decay via photooxidation was also included in the model (Figure 3). The mean estimate of epilimnetic DOC decay rate at 20°C for the best performing model, Model 1, was 0.007 day^{-1} with a 95% CI of 0.005 to 0.009 day^{-1}. The biological DOC decay rates (Figure 3a) varied across the four best performing models, however that was an artifact of adding compensating processes and parameters to the model structure. For instance, Model 3 simulated the effect of both light and microbes, which in turn were implicitly represented through the effect of epilimnetic temperature on DOC decay, whereas Model 1 simulated microbial DOC decay only. The sum of k_{20} and $kbase_{photo}$ in Model 3 was 0.007 day^{-1}—the value of k_{20} in Model 1 (Figures 3a and 3d), and the effect of temperature and light on DOC decay was additive, likely due to significant positive correlation between measured epilimnetic temperature and PAR ($r = 0.4$, $p < 0.001$). Base decay in Model 2 was slightly lower than in Model 1 (by 14%), which would have resulted in higher epilimnetic DOC pools if the DOC transports from the hypolimnion were not reduced by 14% through the parameter u_2 (Figures 3a and 3g and Table S1).

Temperature sensitivity of epilimnetic DOC decay predicted by Model 1 was 1.038 (Figure 3b and Table S1), indicating that a 10°C increase in epilimnion temperature would increase DOC decay rate by 45%. While the temperature sensitivity increased with the addition of processes and parameters among the four best performing models, there was little change in the estimated rate of DOC decay flux because of compensatory decreases in the base decay rate.

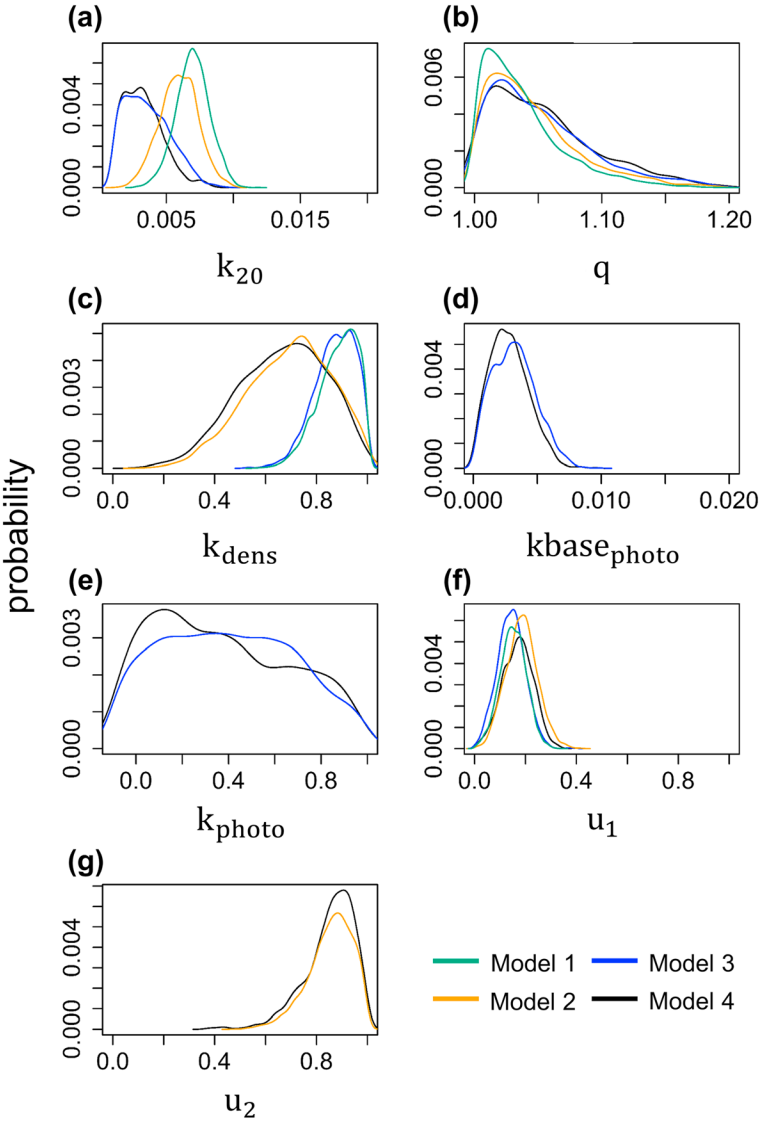

Parameter	Description	Models in which present
k_{20}	decay rate at 20°C, day^{-1}	1,2,3,4
q	temperature sensitivity	1,2,3,4
k_{dens}	sensitivity of C load partitioning to differences in stream and epi water densities	1,2,3,4
$kbase_{photo}$	base photodegradation rate, day^{-1}	3,4
k_{photo}	sensitivity of photodegradation to changes in PAR	3,4
u_1	value between 0 and 1 correcting for depth gradient in hypo DIC	1,2,3,4
u_2	value between 0 and 1 correcting for depth gradient in hypo DOC	2,4

Figure 3. Marginal posterior parameter distributions for the four best fitting models described in equations 1–5 and 11–17 in the supporting information, and the summary of the differences between the four best performing models. Ranges of *x* axes indicate the boundaries of prior uniform distributions.

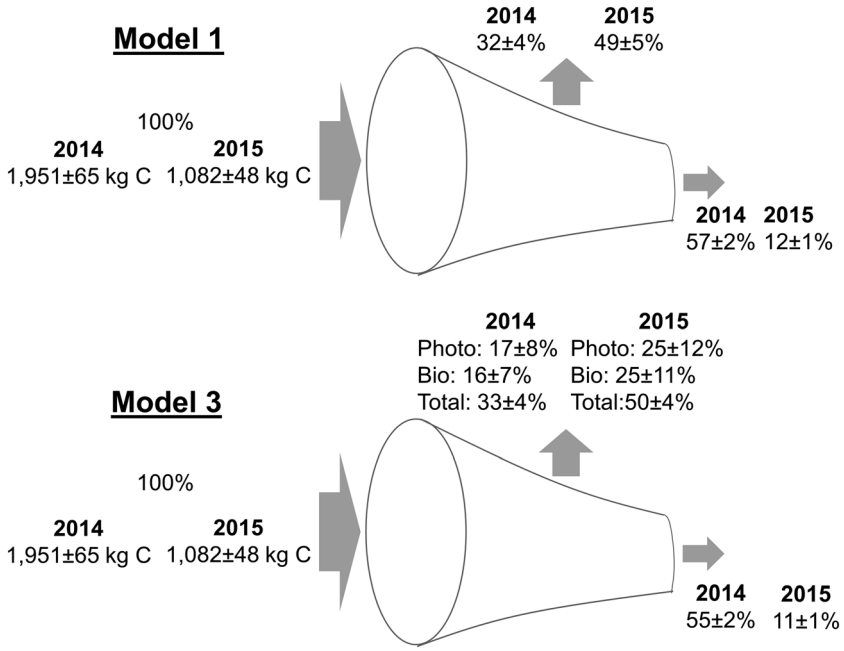

Figure 4. Fate of dissolved organic carbon (DOC) load to epilimnion from late May to early October of 2014 and 2015 simulated by (top) Model 1and (bottom) Model 3. Epilimnetic DOC input was calculated as the sum of exuded fraction of gross primary product, allochthonous DOC partitioned to epilimnion, and entrained hypolimnetic DOC.

3.3.3. Fate of Allochthonous DOC

All four of the best models produced similar estimates of the fate (mineralization, hydrologic export, or storage) of DOC inputs to the lake and demonstrated large differences in DOC fate between 2014 and 2015 that were likely due to interannual differences in precipitation and hydrologic fluxes (Figure 4). In 2014, 88–89% of incoming DOC was mineralized or exported, whereas only 61% was mineralized or exported in 2015. Proportionally, in the wetter year (2014), more C was exported than mineralized, whereas more C was mineralized than exported in the drier year. Drier conditions in 2015 compared to 2014 led to nearly a twofold decrease in epilimnetic DOC load; however, despite the smaller load, nearly twice as much of "fresh" DOC remained in the lake in 2015 (422 kg C) than in 2014 (215–234 kg C).

4. Discussion

4.1. Physical Versus Biochemical Control

Reliable assessment and prediction of seasonal CO_2 emissions from lakes depend in part on accurate understanding of DOC and CO_2 dynamics. Models commonly focus on representing biological controls of DOC and CO_2 dynamics (Bennington et al., 2012; Hanson et al., 2011; Pilcher et al., 2015), often overlooking such physical effects on C dynamics as inflow partitioning between epilimnion and hypolimnion and entrainment (but see Vachon, Prairie, et al., 2017). In our analysis, which included assumptions about various physical and biological drivers of C dynamics, entrainment of vertically heterogeneous hypolimnetic CO_2 was the most important feature of models that represented DOC and CO_2 dynamics well (Figure 1). Entrainment has been shown to affect epilimnetic DO and CO_2 dynamics, mainly by importing anoxic waters rich in CO_2 into the epilimnion (Baehr & DeGrandpre, 2004; Jennings et al., 2012). Moreover, entrainment can be a significant source of nutrients to the epilimnion (MacIntyre et al., 2006) and thus enhance both productivity (Baehr & DeGrandpre, 2004; Giling et al., 2017) and DOC decay rates (Guillemette et al., 2013; Räsänen et al., 2014). The possible entrainment-driven productivity enhancement was indirectly accounted for in our study, because we used observation-based gross primary product as model input. However, we did not account for a possible increase in DOC decay after entrainment of hypolimnetic water, which could have caused underprediction of CO_2 and overprediction of DOC in late September after a series of frequent entrainment events from thermocline deepening.

The density gradient between stream and epilimnetic water could form a gravity-driven density current, which could transport the stream constituents to the hypolimnion (Rueda et al., 2007). The importance of

density currents for nutrient transport into the hypolimnion has been demonstrated for larger lakes and reservoirs (Marcé et al., 2008; Rueda et al., 2007) but has been overlooked in small lakes. In our analysis density-driven import of DOC and CO_2 into the hypolimnion was the second most important predictor of good model performance in simulating epilimnetic C dynamics. The density difference between colder stream and warmer epilimnetic water at East Long Lake exceeded 2.5 kg m^{-3} in summer months, causing as much as 92% of incoming DOC and CO_2 to be partitioned to the hypolimnion. Our results emphasize the importance of accounting for physical processes for accurate representation of C dynamics.

4.2. Base DOC Decay Rates

Our mean estimate of DOC decay at 20°C (0.007 day^{-1} with 95% CI of 0.005 to 0.009 day^{-1}) was similar to though slightly higher than the rate reported by Houser (2001) for lakes near our study lake (0.005 day^{-1}), and subsequently used in some carbon budget models (e.g., Hanson et al., 2004, 2011). In contrast, our estimate was on the low end of the range reported for lakes in southern Quebec (0.0057–0.17 day^{-1}; Guillemette & del Giorgio, 2011). These differences in estimated rates may in part reflect differences in the average lability of carbon among this diverse set of lakes.

4.3. Temperature Sensitivity of DOC Decay

Continuing greenhouse gas emissions and land use change are projected to increase global average temperatures by another 3.8°C by 2,100 (Pachauri et al., 2014), potentially accelerating greenhouse gas emissions from lakes. It has been commonly assumed that with a 10°C increase in temperature, DOC decay rates will double (often expressed as Q10 = 2; Hanson et al., 2004), with some studies assuming a nearly threefold increase in DOC decay rates under similar conditions (Berggren et al., 2010). Recent meta-analysis demonstrated that temperature sensitivities of DOC decay vary widely across lake ecosystems (Yvon-Durocher et al., 2012). The data-informed mean temperature sensitivity of DOC decay in East Long Lake was lower than the means reported in the literature (Hanson et al., 2004, 2011; Miller et al., 2009). During cooler periods, temperature did not inhibit DOC decay as expected from the mean value across various ecosystems, and during warmer periods, increases in DOC decay rates were below the average estimate obtained from in situ lake respiration measurements (Yvon-Durocher et al., 2012). All other conditions being equal, a 3°C increase in average epilimnetic temperature from the current 21.4°C would result in 12 to 20% smaller response in DOC decay than would be expected based on existing literature.

A possible reason for lower temperature sensitivities of DOC decay at Long Lake could be higher average temperatures at our site than in the studies that reported higher Q10s. A negative relationship between respiration Q10 and average temperature has been observed in terrestrial ecosystems (Chen & Tian, 2005; Peng et al., 2009); hence, we tested this hypothesis by calculating in situ Q10s of lake pelagic respiration reported in Yvon-Durocher et al. (2012) and relating them to the average temperatures of the measurement periods (Figure 5b). Data from Yvon-Durocher et al. (2012) yielded a negative exponential relationship between Q10s and the average temperatures. Moreover, the regression coefficients were remarkably close to the ones describing the relationship between soil respiration Q10s and temperature (Figure 2 in Chen & Tian, 2005) in temperate and boreal regions. The Q10 for East Long Lake obtained from the equation in Figure 5b (given that the average epilimnetic temperature at East Long Lake during the measurement period was 21.4°C) was 1.46 and almost identical to the Q10 obtained in this study, which was 1.45.

4.4. Photodegradation of DOC

There is substantial uncertainty in the literature about photomineralization rates and their importance for total DOC mineralization (Cory et al., 2014; Molot & Dillon, 1997; Vachon et al., 2016). In this study photodegradation rates ranged from 0.0034 to 0.0045 day^{-1} with a seasonal average of 0.004 day^{-1} for the period from late May to October, which was within the range reported in the literature (0.0009–0.097 day^{-1}; Molot & Dillon, 1997; Porcal et al., 2014; Vachon et al., 2016). Photodegradation contributed around 50% to total DOC mineralization rates, ranging from 42% during the warmer months to 60% in the days with the lowest epilimnetic temperatures, which was also within the range reported in the literature (14–95%; Granéli et al., 1996; Molot & Dillon, 1997; Vachon et al., 2016).

Although our values for photodegradation rates and their contribution to total DOC mineralization rates agree with some values reported in the literature, we are cautious in interpreting them as true

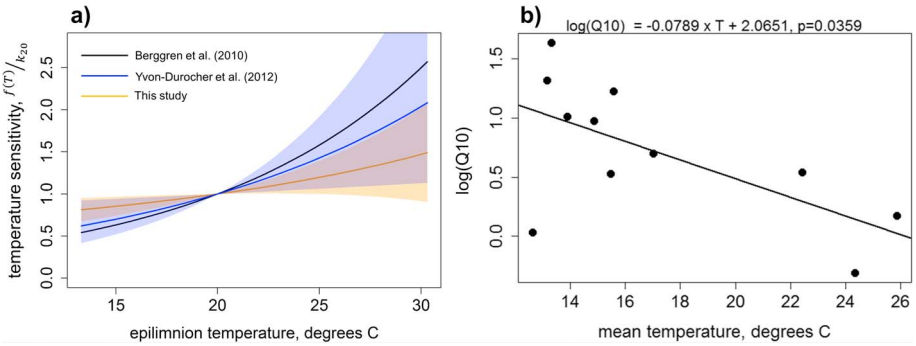

Figure 5. (a) Temperature sensitivity of dissolved organic carbon decay expressed as actual decay rate normalized by the decay rate at T = 20°C and (b) dependency of in situ lake Q10s to temperature. The green line represents maximum likelihood estimates from this study (shaded region is ±1 SD), the red line represents temperature sensitivity used in Berggren et al. (2010), and the blue line represents temperature sensitivities calculated from meta-analysis by Yvon-Durocher et al. (2012), with shaded regions representing ±1 SD of Q10s calculated for in situ lake pelagic respiration measurements. Relationship in (b) was derived from calculating in situ Q10s for lake pelagic respiration from data in Yvon-Durocher et al. (2012).

photomineralization rates. Our caution stems from the lack of significant improvement in model performance that we observed when including photooxidation in the models (Figure 1) and from equifinality in model performance. The equifinality was evident from the additivity of biodegradation and photodegradation rates (see section 3.3.2) and the equal split of mineralized DOC between photodegradation and biodegradation with nonadditive uncertainties (Figure 4), which was likely due to significant positive correlation between PAR and epilimnetic temperature (r = 0.4, $p < 0.001$). Accurately representing photodegradation is important when simulating C dynamics at hourly timesteps: lake respiration may be overestimated at night, for example, by Model 1, when the temperature coefficient also implicitly accounts for the light effect on DOC decay. It is also particularly important to accurately capture photodegradation rates in northern lakes, which may have substantial rates of CO_2 efflux despite low temperatures (Cory et al., 2014; Solomon et al., 2013). A potential way to estimate photomineralization rates more reliably would be to extend the measurement season into spring and fall to include C dynamics under low temperatures but relatively high PAR conditions and repeat the calibration analysis with the new data. Alternatively, photodegradation rates in East Long Lake could be constrained via in situ incubation experiment as in Molot and Dillon (1997).

4.5. DOC Recalcitrance

DOC is composed of many molecules of varying lability (del Giorgio & Davis, 2003; Guillemette & del Giorgio, 2011; Middelburg et al., 1993), and many aquatic C models have sought to incorporate this heterogeneity by including two or more DOC pools of differing lability. In contrast, our study showed that partitioning the DOC pool into labile and recalcitrant fractions did not yield significant improvements in model fits to the observed DOC and CO_2 (Figure 1). The disagreement between our results and the literature is likely due to modeling and observing different systems: long-term incubation versus in situ lakes. Indeed, if we simulate a DOC incubation experiment using a model with one and two DOC pools, the DOC decay dynamics will be slightly distinct between the two models. The two-pool model will have two stages of DOC decay: a rapid initial stage and a slower later stage, which will not align with the exponential decay pattern of the one-pool model. Models with one and two DOC pools also differed in simulating DOC fate, with two-pool models simulating slightly higher mineralization that resulted from the rapid initial decay of the labile DOC fraction. At East Long Lake, the estimated initial fraction of labile DOC and labile fraction of DOC loads were small, 10% and 25%, respectively; hence, the differences in short-term fates of incoming DOC were small. We speculate that for lakes with higher labile DOC inputs, the differences between one and two DOC pool models will be more pronounced, and the two-pool model may perform significantly better.

5. Conclusion

Our formal data assimilation approach allowed us to evaluate a diverse set of hypothesized drivers of lake carbon biogeochemistry and the physical, chemical, and biological interactions among these drivers. By

leveraging process models and data collected at the ecosystem scale, we were able to identify system-scale processes that cannot be captured in traditional incubation studies, including the importance of hypolimnetic entrainment and density-driven sinking of terrestrial hydrologic loads, as most important for predicting seasonal dynamics of lake carbon biogeochemistry. Although system-scale physical processes were most important, temperature dependence of carbon decomposition was also present in our best models. However, model calibration revealed a weaker sensitivity of organic matter decay to temperature than is commonly assumed. Application of these approaches in a comparative framework across regions will be an important next step for evaluating the generality of our findings, but our work indicates great promise for reliable forecasting of intraannual lake carbon biogeochemistry dynamics.

Acknowledgments

We thank the University of Notre Dame Environmental Research Center for hosting our study. The chemical analyses were conducted at the Center for Environmental Science and Technology at University of Notre Dame. Synthetic data assimilation analyses were run with the support of Notre Dame's Center for Research Computing. Technical assistance was provided by J. J. Coloso, B. Conner, S. McCarthy, E. Mather, S. Elser, C. J. Humes, J. Lerner, and M. F. Ebenezer. Our work on this project was supported by a team grant from the Fonds de recherche du Québec-nature et technologies (FRQNT 191167) to C. T. S., Y. T. P., and P. del Giorgio, and also supported by the National Science Foundation Graduate Research Fellowship under NSF DGE-1313583 to J. A. Z. and NSF award DEB-1547866 to S. E. J. We also thank two anonymous reviewers for their contributions to improvement of this manuscript. The authors declare no financial conflicts of interest. The scripts and data used in this study are located at https://github.com/MFEh2o/Hararuk_DA.

References

Akaike, H. (1974). A new look at the statistical model identification. *IEEE Transactions on Automatic Control*, *19*(6), 716–723. https://doi.org/10.1109/TAC.1974.1100705

Amado, A. M., Farjalla, V. F., Esteves, F. A., & Bozelli, R. L. (2003). DOC photo-oxidation in clear water Amazonian aquatic ecosystems. *Amazoniana*, *17*(3–4), 513–523.

Baehr, M. M., & DeGrandpre, M. D. (2004). In situ pCO_2 and O_2 measurements in a lake during turnover and stratification: Observations and modeling. *Limnology and Oceanography*, *49*(2), 330–340. https://doi.org/10.4319/lo.2004.49.2.0330

Bennington, V., McKinley, G. A., Urban, N. R., & McDonald, C. P. (2012). Can spatial heterogeneity explain the perceived imbalance in Lake Superior's carbon budget? A model study. *Journal of Geophysical Research*, *117*, G03020. https://doi.org/10.1029/2011JG001895

Berggren, M., Ström, L., Laudon, H., Karlsson, J., Jonsson, A., Giesler, R., et al. (2010). Lake secondary production fueled by rapid transfer of low molecular weight organic carbon from terrestrial sources to aquatic consumers. *Ecology Letters*, *13*(7), 870–880. https://doi.org/10.1111/j.1461-0248.2010.01483.x

Besag, J., Green, P., Higdon, D., & Mengersen, K. (1995). Bayesian computation and stochastic systems. *Statistical Science*, *10*(1), 3–41. https://doi.org/10.1214/ss/1177010123

Bouwer, H. (1989). The Bouwer and Rice Slug Test — An Updatea. *Groundwater*, *27*, 304–309.

Bower, P., & McCorkle, D. (1980). Gas exchange, photosynthetic uptake, and carbon budget for a radiocarbon addition to a small enclosure in a stratified Lake. *Canadian Journal of Fisheries and Aquatic Sciences*, *37*(3), 464–471. https://doi.org/10.1139/f80-060

Cardille, J. A., Carpenter, S. R., Coe, M. T., Foley, J. A., Hanson, P. C., Turner, M. G., & Vano, J. A. (2007). Carbon and water cycling in lake-rich landscapes: Landscape connections, lake hydrology, and biogeochemistry. *Journal of Geophysical Research*, *112*, G02031. https://doi.org/10.1029/2006JG000200

Chen, H., & Tian, H.-Q. (2005). Does a general temperature-dependent Q10 model of soil respiration exist at biome and global scale? *Journal of Integrative Plant Biology*, *47*(11), 1288–1302. https://doi.org/10.1111/j.1744-7909.2005.00211.x

Cory, R. M., Ward, C. P., Crump, B. C., & Kling, G. W. (2014). Sunlight controls water column processing of carbon in arctic fresh waters. *Science*, *345*(6199), 925–928. https://doi.org/10.1126/science.1253119

Daugherty, R. L., & Ingersoll, A. C. (1954). *Fluid Mechanics, with Engineering Applications*. New York: McGraw-Hill.

del Giorgio, P. A., & Davis, J. (2003). 17 - Patterns in dissolved organic matter Lability and consumption across aquatic ecosystems A2 - Findlay, Stuart E.G. In R. L. Sinsabaugh (Ed.), *Aquatic Ecosystems* (pp. 399–424). Burlington: Academic Press. https://doi.org/10.1016/B978-012256371-3/50018-4

Einola, E., Rantakari, M., Kankaala, P., Kortelainen, P., Ojala, A., Pajunen, H., et al. (2011). Carbon pools and fluxes in a chain of five boreal lakes: A dry and wet year comparison. *Journal of Geophysical Research*, *116*, GO3009. https://doi.org/10.1029/2010JG001636

Fahrner, S., Radke, M., Karger, D., & Blodau, C. (2008). Organic matter mineralisation in the hypolimnion of an eutrophic Maar lake. *Aquatic Sciences*, *70*(3), 225–237. https://doi.org/10.1007/s00027-008-8008-2

Gelman, A., Roberts, G., & Gilks, W. (1996). Efficient metropolis jumping rules. In J. M. Bernardo, J. O. Berger, A. P. Dawid, & A. F. M. Smith (Eds.), *Bayesian Statistics* (pp. 599–607). Oxford: Oxford University Press.

Giling, D. P., Nejstgaard, J. C., Berger, S. A., Grossart, H.-P., Kirillin, G., Penske, A., et al. (2017). Thermocline deepening boosts ecosystem metabolism: Evidence from a large-scale lake enclosure experiment simulating a summer storm. *Global Change Biology*, *23*(4), 1448–1462. https://doi.org/10.1111/gcb.13512

Granéli, W., Lindell, M., & Tranvik, L. (1996). Photo-oxidative production of dissolved inorganic carbon in lakes of different humic content. *Limnology and Oceanography*, *41*(4), 698–706. https://doi.org/10.4319/lo.1996.41.4.0698

Guillemette, F., & del Giorgio, P. A. (2011). Reconstructing the various facets of dissolved organic carbon bioavailability in freshwater ecosystems. *Limnology and Oceanography*, *56*(2), 734–748. https://doi.org/10.4319/lo.2011.56.2.0734

Guillemette, F., McCallister, S. L., & del Giorgio, P. A. (2013). Differentiating the degradation dynamics of algal and terrestrial carbon within complex natural dissolved organic carbon in temperate lakes. *Journal of Geophysical Research: Biogeosciences*, *118*, 963–973. https://doi.org/10.1002/jgrg.20077

Haario, H., Saksman, E., & Tamminen, J. (2001). An adaptive metropolis algorithm. *Bernoulli*, *7*(2), 223–242. https://doi.org/10.2307/3318737

Hanson, P. C., Hamilton, D. P., Stanley, E. H., Preston, N., Langman, O. C., & Kara, E. L. (2011). Fate of allochthonous dissolved organic carbon in lakes: A quantitative approach. *PLoS One*, *6*(7), e21884. https://doi.org/10.1371/journal.pone.0021884

Hanson, P. C., Pollard, A. I., Bade, D. L., Predick, K., Carpenter, S. R., & Foley, J. A. (2004). A model of carbon evasion and sedimentation in temperate lakes. *Global Change Biology*, *10*(8), 1285–1298. https://doi.org/10.1111/j.1529-8817.2003.00805.x

Hothorn, T., Hornik, K., & Zeileis, A. (2006). Unbiased recursive partitioning: A conditional inference framework. *Journal of Computational and Graphical Statistics*, *15*(3), 651–674. https://doi.org/10.1198/106186006X133933

Hothorn, T., Hornik, K., & Zeileis, A. (2015). ctree: Conditional inference trees, *cran. r_project*.

Houser, J. N. (2001). Dissolved organic carbon in lakes: Effects on thermal structure, primary production, and hypolimnetic metabolism. University of Wisconsin at Madison (USA).

Jennings, E., Jones, S., Arvola, L., Staehr, P. A., Gaiser, E., Jones, I. D., et al. (2012). Effects of weather-related episodic events in lakes: An analysis based on high-frequency data. *Freshwater Biology*, *57*(3), 589–601. https://doi.org/10.1111/j.1365-2427.2011.02729.x

Kelly, C. A., Fee, E., Ramlal, P. S., Rudd, J. W. M., Hesslein, R. H., Anema, C., & Schindler, E. U. (2001). Natural variability of carbon dioxide and net epilimnetic production in the surface waters of boreal lakes of different sizes. *Limnology and Oceanography*, *46*(5), 1054–1064. https://doi.org/10.4319/lo.2001.46.5.1054

Kelly, P. T., Craig, N., Solomon, C. T., Weidel, B. C., Zwart, J. A., & Jones, S. E. (2016). Experimental whole-lake increase of dissolved organic carbon concentration produces unexpected increase in crustacean zooplankton density. *Global Change Biology*, *22*(8), 2766–2775. https://doi.org/10.1111/gcb.13260

Le Quéré, C., Andrew, R. M., Canadell, J. G., Sitch, S., Korsbakken, J. I., Peters, G. P., & Manning, A. C. (2016). Global carbon budget 2016. *Earth System Science Data*, *8*(2), 605–649. https://doi.org/10.5194/essd-8-605-2016

MacIntyre, S., Sickman, J. O., Goldthwait, S. A., & Kling, G. W. (2006). Physical pathways of nutrient supply in a small, ultraoligotrophic arctic lake during summer stratification. *Limnology and Oceanography*, *51*(2), 1107–1124. https://doi.org/10.4319/lo.2006.51.2.1107

Marcé, R., Moreno-Ostos, E., & Armengol, J. (2008). The role of river inputs on the hypolimnetic chemistry of a productive reservoir: Implications for management of anoxia and total phosphorus internal loading. *Lake and Reservoir Management*, *24*(1), 87–98. https://doi.org/10.1080/07438140809354053

Middelboe, M., & Lundsgaard, C. (2003). Microbial activity in the Greenland Sea: Role of DOC lability, mineral nutrients and temperature. *Aquatic Microbial Ecology*, *32*(2), 151–163. https://doi.org/10.3354/ame032151

Middelburg, J. J., Vlug, T., Jaco, F., & van der Nat, W. A. (1993). Organic matter mineralization in marine systems. *Global and Planetary Change*, *8*(1-2), 47–58. https://doi.org/10.1016/0921-8181(93)90062-S

Miller, M. P., McKnight, D. M., Chapra, S. C., & Williams, M. W. (2009). A model of degradation and production of three pools of dissolved organic matter in an alpine lake. *Limnology and Oceanography*, *54*(6), 2213–2227. https://doi.org/10.4319/lo.2009.54.6.2213

Molot, L. A., & Dillon, P. J. (1997). Photolytic regulation of dissolved organic carbon in northern lakes. *Global Biogeochemical Cycles*, *11*, 357–365. https://doi.org/10.1029/97GB01198

Moore, R. D. (2005). Slug injection using salt in solution. *Streamline Watershed Management Bulletin*, *8*(2), 1–6.

Pachauri, R. K., Allen, M. R., Barros, V. R., Broome, J., Cramer, W., Christ, R., et al. (2014). *Climate change 2014: synthesis report. Contribution of Working Groups I, II and III to the fifth assessment report of the Intergovernmental Panel on Climate Change*, IPCC.

Peng, S., Piao, S., Wang, T., Sun, J., & Shen, Z. (2009). Temperature sensitivity of soil respiration in different ecosystems in China. *Soil Biology and Biochemistry*, *41*(5), 1008–1014. https://doi.org/10.1016/j.soilbio.2008.10.023

Pilcher, D. J., McKinley, G. A., Bootsma, H. A., & Bennington, V. (2015). Physical and biogeochemical mechanisms of internal carbon cycling in Lake Michigan. *Journal of Geophysical Research: Oceans*, *120*, 2112–2128. https://doi.org/10.1002/2014JC010594

Porcal, P., Dillon, P. J., & Molot, L. A. (2014). Interaction of extrinsic chemical factors affecting photodegradation of dissolved organic matter in aquatic ecosystems. *Photochemical & Photobiological Sciences*, *13*(5), 799–812. https://doi.org/10.1039/C4PP00011K

Räsänen, N., Kankaala, P., Tahvanainen, T., Akkanen, J., & Saarnio, S. (2014). Short-term effects of phosphorus addition and pH rise on bacterial utilization and biodegradation of dissolved organic carbon (DOC) from boreal mires. *Aquatic Ecology*, *48*(4), 435–446. https://doi.org/10.1007/s10452-014-9496-x

Raymond, P. A., Hartmann, J., Lauerwald, R., Sobek, S., McDonald, C., Hoover, M., et al. (2013). Global carbon dioxide emissions from inland waters. *Nature*, *503*(7476), 355–359. https://doi.org/10.1038/nature12760, https://www.nature.com/articles/nature12760#supplementary-information

Rinta, P., Bastviken, D., van Hardenbroek, M., Kankaala, P., Leuenberger, M., Schilder, J., et al. (2015). An inter-regional assessment of concentrations and δ13C values of methane and dissolved inorganic carbon in small European lakes. *Aquatic Sciences*, *77*(4), 667–680. https://doi.org/10.1007/s00027-015-0410-y

Rueda, F. J., Fleenor, W. E., & de Vicente, I. (2007). Pathways of river nutrients towards the euphotic zone in a deep-reservoir of small size: Uncertainty analysis. *Ecological Modelling*, *202*(3–4), 345–361. https://doi.org/10.1016/j.ecolmodel.2006.11.006

Shiller, A. M., Duan, S., van Erp, P., & Bianchi, T. S. (2006). Photo-oxidation of dissolved organic matter in river water and its effect on trace element speciation. *Limnology and Oceanography*, *51*(4), 1716–1728. https://doi.org/10.4319/lo.2006.51.4.1716

Solomon, C. T., Bruesewitz, D. A., Richardson, D. C., Rose, K. C., van de Bogert, M. C., Hanson, P. C., et al. (2013). Ecosystem respiration: Drivers of daily variability and background respiration in lakes around the globe. *Limnology and Oceanography*, *58*(3), 849–866. https://doi.org/10.4319/lo.2013.58.3.0849

Spall, J. C. (2005). *Introduction to stochastic search and optimization: estimation, simulation, and control*. Hoboken, NJ: John Wiley & Sons.

Stumm, W., & Morgan, J. J. (1981). *Aquatic chemistry: An introduction emphasizing chemical equilibria in natural waters*. New York: Wiley.

Tranvik, L. J., Downing, J. A., Cotner, J. B., Loiselle, S. A., Striegl, R. G., Ballatore, T. J., et al. (2009). Lakes and reservoirs as regulators of carbon cycling and climate. *Limnology and Oceanography*, *54*(6part2), 2298–2314. https://doi.org/10.4319/lo.2009.54.6_part_2.2298

Vachon, D., & del Giorgio, P. A. (2014). Whole-Lake CO_2 dynamics in response to storm events in two morphologically different lakes. *Ecosystems*, *17*(8), 1338–1353. https://doi.org/10.1007/s10021-014-9799-8

Vachon, D., Lapierre, J.-F., & del Giorgio, P. A. (2016). Seasonality of photochemical dissolved organic carbon mineralization and its relative contribution to pelagic CO_2 production in northern lakes. *Journal of Geophysical Research: Biogeosciences*, *121*, 864–878. https://doi.org/10.1002/2015JG003244

Vachon, D., Prairie, Y. T., Guillemette, F., & del Giorgio, P. A. (2017). Modeling Allochthonous dissolved organic carbon mineralization under variable hydrologic regimes in boreal lakes. *Ecosystems*, *20*(4), 781–795. https://doi.org/10.1007/s10021-016-0057-0

Vachon, D., Solomon, C. T., & del Giorgio, P. A. (2017). Reconstructing the seasonal dynamics and relative contribution of the major processes sustaining CO_2 emissions in northern lakes. *Limnology and Oceanography*, *62*(2), 706–722. https://doi.org/10.1002/lno.10454

Xu, T., White, L., Hui, D., & Luo, Y. (2006). Probabilistic inversion of a terrestrial ecosystem model: Analysis of uncertainty in parameter estimation and model prediction. *Global Biogeochemical Cycles*, *20*, GB2007. https://doi.org/10.1029/2005GB002468

Yvon-Durocher, G., Caffrey, J. M., Cescatti, A., Dossena, M., Giorgio, P., Gasol, J. M., et al. (2012). Reconciling the temperature dependence of respiration across timescales and ecosystem types. *Nature*, *487*(7408), 472–476. http://www.nature.com/nature/journal/v487/n7408/abs/nature11205.html#supplementary-information, https://doi.org/10.1038/nature11205

Zwart, J. A., Craig, N., Kelly, P. T., Sebestyen, S. D., Solomon, C. T., Weidel, B. C., & Jones, S. E. (2016). Metabolic and physiochemical responses to a whole-lake experimental increase in dissolved organic carbon in a north-temperate lake. *Limnology and Oceanography*, *61*(2), 723–734. https://doi.org/10.1002/lno.10248

Zwart, J. A., Sebestyen, S. D., Solomon, C. T., & Jones, S. E. (2017). The influence of hydrologic residence time on Lake carbon cycling dynamics following extreme precipitation events. *Ecosystems*, *20*(5), 1000–1014. https://doi.org/10.1007/s10021-016-0088-6